

5.4

RAMAN LIDAR MEASUREMENTS OF AEROSOL AND WATER VAPOR OVER THE SOUTHERN GREAT PLAINS

Richard Ferrare*

NASA Langley Research Center, Hampton, Virginia

David Turner

Pacific Northwest National Lab, P.O. Box 999/K9-24, Richland, Washington

Marian Clayton

SAIC, Hampton, Virginia

Dave Covert, Robert Elleman

Department of Atmospheric Sciences, University of Washington, Seattle, Washington

Hafliði Jonsson

CIRPAS/Naval Postgraduate School, 3200 Imjin Road, Marina, California

Beat Schmid, Jens Redemann

BAER/NASA Ames Research Institute, MS 245-5, Moffett Field, California

John Ogren, Elisabeth Andrew

NOAA/CMDL, 325 Broadway R/CMDL1, Boulder, Colorado

Mian Chin

NASA Goddard Space Flight Center, Code 916, Greenbelt, Maryland

Ian Brooks

School of Earth and Environment, University of Leeds, Leeds

Sarah Guibert, Michael Schultz

Laboratoire des Sciences du Climat et de l'Environnement, CEA/CNRS-LSCE, France

1. INTRODUCTION

Measurements of aerosol optical properties are required to meet two of the primary objectives of the Department of Energy Atmospheric Radiation Measurement (ARM) Program, which are: 1) relate observations of radiative fluxes and radiances to the atmospheric composition and, 2) use these relations to develop and test parameterizations to accurately predict the atmospheric radiative properties. Consequently, ARM has developed the Climate Research Facility (CART) Raman lidar (CARL), which operates as a turnkey, automated system for unattended, around-the-clock profiling of water vapor and aerosols over the Southern Great Plains Climate Research Facility (Goldsmith et al., 1998). We describe how these lidar profiles are used to

evaluate aerosol model simulations, evaluate the vertical variability and distribution of aerosols, and retrieve aerosol optical properties.

2. RAMAN LIDAR SYSTEM

CARL autonomously measures profiles of aerosols, clouds and water vapor in the low to mid troposphere throughout the diurnal cycle. A tripled Nd:YAG laser, operating at 30 Hz with 350-400 millijoule pulses, is used to transmit light at 355 nm. A telescope collects the light backscattered by molecules and aerosols at the laser wavelength and the Raman scattered light from water vapor (408 nm) and nitrogen (387 nm) molecules. Profiles of water vapor mixing ratio, relative humidity, aerosol backscattering, and aerosol extinction are derived routinely using a set of automated algorithms (Turner et al., 2002). Water vapor mixing ratio profiles are computed using the ratio of the Raman water vapor signal to the Raman nitrogen signal. Relative humidity profiles are computed using these profiles and the

*Corresponding author address: NASA Langley Research Center, Mail Stop 401A, Hampton, Virginia, 23681, USA, richard.a.ferrare@nasa.gov

temperature profiles from a collocated Atmospheric Emitted Radiance Interferometer (AERI). The water vapor mixing ratio profiles are integrated with altitude to derive precipitable water vapor (PWV). Profiles of aerosol scattering ratio are derived using the Raman nitrogen signal and the signal detected at the laser wavelength. Aerosol volume backscattering cross section profiles are then computed using the aerosol scattering ratio and molecular scattering cross section profiles derived from atmospheric density data. Aerosol extinction profiles are computed from the derivative of the logarithm of the Raman nitrogen signal with respect to range. Aerosol optical thickness (AOT) is derived by integration of the aerosol extinction profile with altitude.

3. COMPARISONS WITH AEROSOL MODELS

These Raman lidar aerosol extinction profiles were used to evaluate aerosol extinction profiles and aerosol optical thickness (AOT) simulated by the Georgia Tech/Goddard Global Ozone Chemistry Aerosol Radiation and Transport (GOCART) and Interaction with Chemistry and Aerosols (INCA) global aerosol models' simulations for the year 2000. The GOCART and INCA model average aerosol extinction profiles show good agreement with the Raman lidar profiles for altitudes above about 2 km; below 2 km the average model profiles are significantly (30-50%) lower than the Raman lidar profiles. The vertical variability in average aerosol extinction profiles simulated by these models is less than the variability in the corresponding Raman lidar profiles.

4. PBL RETRIEVALS

PBL heights and transition zone thicknesses were derived from Raman lidar water vapor and aerosol profiles acquired over the period between January 2000 and December 2002. These parameters were derived using a robust and objective method that uses the Haar wavelet covariance transform with multiple dilations (Brooks, 2003). The PBL heights derived from the Raman lidar measurements were compared with the PBL heights computed from potential temperature profiles derived from simultaneous radiosonde measurements. The agreement among the heights derived from the various profiles varies with conditions. At night there are substantial differences due to the lidar sensitivity to residual aerosol and water vapor layers above the height of the temperature inversion. Results

from this day and for this entire period indicate that these techniques are in much better agreement for profiles acquired during the afternoon and early evening. The PBL heights were also used to evaluate the amount of aerosol optical thickness within and above the boundary layer. These results indicated that a significant fraction (>25%) of aerosol optical thickness is above the PBL; this amount varies with time of day, but does not significantly change with season or aerosol optical thickness.

5. RETRIEVALS OF AEROSOL SINGLE SCATTER ALBEDO AND REFRACTIVE INDEX

During the May 2003 Aerosol IOP, a combination of active (lidar) and passive (Sun photometer) measurements were used along with in situ measurements of the aerosol size distribution to retrieve estimates of the aerosol single scatter albedo and the effective complex refractive index. The aerosol size distributions measured by a PMS Passive Cavity Airborne Spectrometer Probe (PCASP), which measured the number of particles in twenty size bins covering particle diameters between 0.1 and 3 μm , were used in a series of Mie computations to compute the aerosol extinction/backscattering ratio (S_a) and aerosol extinction coefficient. The lidar measurements of S_a (355 nm) and the Angstrom exponents (\AA) that were computed using the aerosol extinction profiles at 450 nm and 675 nm retrieved from the NASA Ames Airborne Tracking 14-channel Sun photometer (AATS14) measurements were used to constrain the retrievals of refractive index and aerosol single scatter albedo. Because higher uncertainties were associated with CARL retrievals acquired during low aerosol extinction conditions, only those cases when the aerosol extinction coefficients were greater than 0.1 km^{-1} were considered. The values of aerosol single scattering albedo (ω_0) derived using this method were found to be in good agreement with values of ω_0 derived from in situ measurements of aerosol scattering and absorption; ω_0 varied between 0.91-0.98; real refractive index (m_r) varied between 1.48-1.60 and imaginary refractive index (m_i) varied between 0.002 to 0.007.

An example of these results for data acquired during May 25 is shown in Figure 1. The aerosol extinction profiles derived from CARL, airborne in situ (nephelometer scattering+PSAP absorption), and AATS14 measurements are shown along with measured and derived aerosol optical properties. Satellite imagery and back trajectory analyses

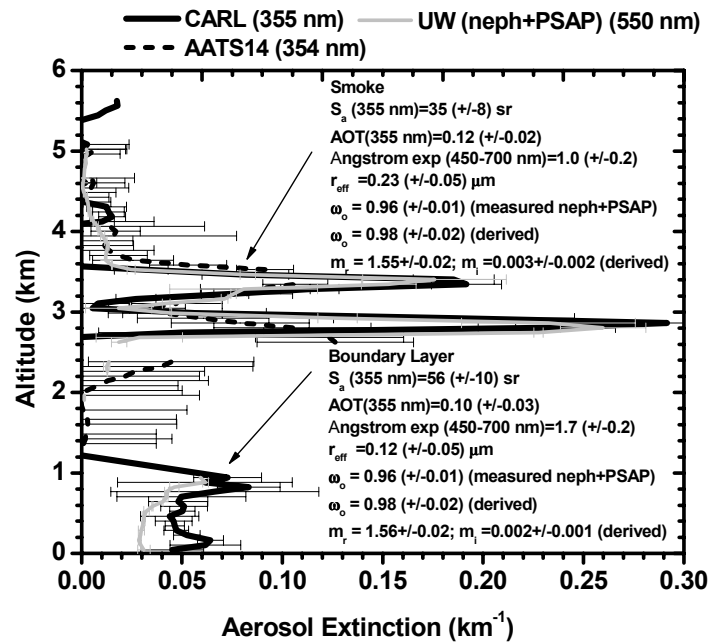


Figure. 1. Aerosol extinction profiles derived from Raman lidar (CARL), airborne Sun photometer (AATS14), and in situ (neph+PSAP) measurements acquired on May 25, 2003 over the ARM SGP site. Measured (S_a , AOT, \AA , r_{eff} , ω_o) and derived (ω_o , m_r , m_i) aerosol properties for smoke and boundary layer aerosols are also shown.

indicate that the elevated aerosol layers located between about 2.6 and 3.6 km were smoke layers produced by Siberian forest fires. The airborne measurements and lidar retrievals indicated that the smoke layers were primarily composed of relatively large particles ($r_{\text{eff}} \sim 0.23 \mu\text{m}$), and that the layers were relatively non-absorbing ($\omega_o \sim 0.96\text{-}0.98$). These results are shown to be consistent with other lidar observations of these smoke layers over Tokyo, Japan and central Europe (Mattis et al., 2004; Muryama et al., 2004).

6. ACKNOWLEDGEMENTS

SGP CART Raman lidar data were obtained from the Atmospheric Radiation Measurement (ARM) Program sponsored by the U.S. Department of Energy, Office of Energy Research, Office of Health and Environmental Research, Environmental Sciences Division. The DOE ARM Program provided funding for this work and for the May 2003 Aerosol IOP.

7. REFERENCES

Brooks, I., 2003: Finding Boundary Layer Top: Application of a Wavelet Covariance Transform to Lidar Backscatter Profiles, *J. Atmos. Oceanic Tech.*, 20, 1092-1105.

Goldsmith, J.E.M. et al., 1998: Turn-Key Raman lidar for profiling atmospheric water vapor, clouds, and aerosols". *Appl. Opt.*, 37, 4979-4990.

Turner, D.D. et al., Automated Retrievals of Water Vapor and Aerosol Profiles over Oklahoma from an Operational Raman Lidar, 2002: *J. Atmos. Oceanic Tech.*, 19, 37-50.

Murayama, T. et al., 2004: Optical Characteristics of Dust and Smoke Aerosols Observed with Multi-wavelength Raman Lidar in Tokyo", 22nd International Laser Radar Conference, G. Pappalardo and A. Amodeo, eds., pp. 365-368.

Mattis, I. et al., 2004: Siberian Forest-Fire Smoke Observed over Central Europe in Spring/Summer 2003 in the Framework of EARLINET", 22nd International Laser Radar Conference, G. Pappalardo and A. Amodeo, eds., pp. 857-860.